

# Numerical simulation of Pacific water intrusions into Otsuchi Bay, northeast of Japan, with a nested-grid OGCM

Takashi T. Sakamoto<sup>1</sup> · L. Shogo Urakawa<sup>2</sup> · Hiroyasu Hasumi<sup>1</sup> · Miho Ishizu<sup>1</sup> · Sachihiko Itoh<sup>1</sup> · Teruhisa Komatsu<sup>1</sup> · Kiyoshi Tanaka<sup>1</sup>

Received: 25 December 2014 / Revised: 8 December 2015 / Accepted: 14 December 2015 / Published online: 22 January 2016  
© The Oceanographic Society of Japan and Springer Japan 2016

**Abstract** A numerical simulation of Otsuchi Bay located on the northeast coast of the Honshu, the largest island of Japan, is conducted, using an ocean general circulation model (OGCM) with a nested-grid system in order to illustrate seasonal variability of the circulation in the bay. Through a year, an anticlockwise circulation is dominant in the bay, as observational studies have implied, although it is modified in the bay-mouth-half of the bay in winter. In addition, there is an intense outflow at the surface layer during spring to autumn, influenced by river water discharge. Intrusion of the Pacific water into the bay is influenced by mean circulations, but it is also influenced by baroclinic tides from spring to autumn. Pacific water intrusions affected by baroclinic tides may have an impact on the environment in Otsuchi Bay.

**Keywords** Baroclinic tide · Sanriku coast · High-resolution numerical model · River discharge · Climatological circulation

## 1 Introduction

Otsuchi Bay is a narrow inlet located on the northeast coast of Japan that runs east–west, is 8 km long and 2 km wide, and opens to the North Pacific on the east (Fig. 1). The huge tsunami caused by the 2011 off the Pacific coast of Tohoku Earthquake, which rushed into the northeast coast and damaged the entire coast on 11 March 2011, also caused massive damage to the ecosystem and aquaculture equipment in Otsuchi Bay. Since the disaster, fishery people and researchers have been concerned as to whether the ecosystem in the bay is recovered to the state before the disaster or changed to a different one. In order to observe the recovering or changing processes of the ecosystem in the bay, several observation lines were set and almost bi-monthly observation has been performed (e.g. Fukuda et al. 2015; Nishibe et al. 2015).

To understand the observed physical, chemical and biological characteristics in Otsuchi Bay, it is important to comprehend water circulation and mixing processes. Before the disaster, sporadic observations were performed in the International Coastal Research Center (ICRC) (e.g. Otobe et al. 1979, 1996). However, details of physical processes in the bay have not been previously studied. Otobe et al. (2009) moored three acoustic Doppler current profilers (ADCPs) on the sea floor from south to north in the center of the bay for almost a year, and illustrated a schematic view of seasonal circulations (residuals): in late fall and winter, westerly or northwesterly winds prevail and an estuary-like circulation, in which an eastward surface outflow and the compensating westward inflow in middle and bottom layers is dominant in the bay. In spring and summer, inflow was observed in the northern side of the bay, and the outflow was observed in the southern one, respectively.

---

**Electronic supplementary material** The online version of this article (doi:[10.1007/s10872-015-0344-y](https://doi.org/10.1007/s10872-015-0344-y)) contains supplementary material, which is available to authorized users.

---

✉ Takashi T. Sakamoto  
teng@aori.u-tokyo.ac.jp

<sup>1</sup> Atmosphere and Ocean Research Institute (AORI),  
The University of Tokyo, 5-1-5 Kashiwanoha, Kashiwa,  
Chiba 277-8568, Japan

<sup>2</sup> Meteorological Research Institute, Japan Meteorological Agency, 1-1 Nagamine, Tsukuba, Ibaraki 305-0052, Japan

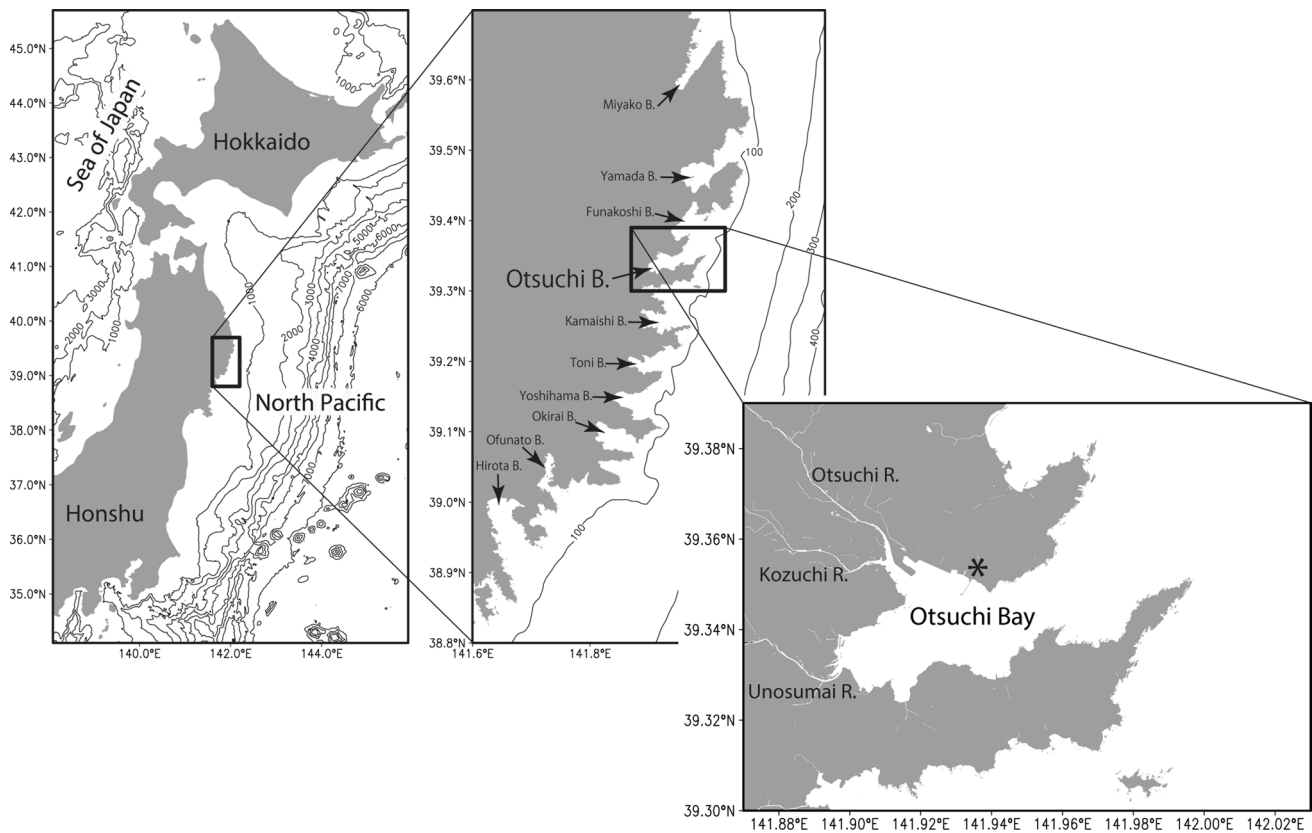


**Fig. 1** Map of Otsuchi Bay, where the target to simulate numerically in the present study is located. Asterisk in the right panel shows the location of the International Coastal Research Center (ICRC). To draw this figure, SRTM30\_PLUS and GSI 10-m mesh elevation data sets are used

Kawamiya et al. (1996) and Kishi et al. (2003) performed numerical simulations of the phytoplankton blooming in spring. Their results showed only an estuary-like circulation, but it was probably difficult for them to discuss the horizontal circulation in the bay, because of the grid size of their model.

Along the northeast coast where Otsuchi Bay is located, the Tsugaru Warm Current, which is a branch of the Tsushima Warm Current in the Sea of Japan flowing through the Tsugaru Strait, usually flows and conveys the warm/saline Tsugaru Warm Water (e.g. Yasuda et al. 1988). Off the coast and beneath the Tsugaru Warm Water, there is the cold/less-saline Oyashio Water. Otsuchi Bay is influenced by the Tsugaru Warm Water throughout the year, but the existence of the Oyashio Water has repeatedly been observed in the bottom layer of the bay (Okazaki 1987; Ishizu et al. unpublished). Although it has been expected that the Oyashio Water intrusion into the bay is caused by internal tides propagating from off the coast, it has not been clarified by the previous observational or numerical studies. In order to know the influences of the waters in the North Pacific on Otsuchi Bay, therefore, an incorporated modeling from a scale of the North Pacific to one of Otsuchi Bay is required.

A purpose of the present study is to illustrate the circulation system in Otsuchi Bay, using a high-resolution and nested grid ocean general circulation model (OGCM), in order to provide basic physical information to understand observed physical, chemical, and biological data in the bay. Noteworthy in this study is a high-resolution modeling in the bay with an O (10 m) gridding, and its incorporation with the basin scale model results. Our model results are discussed by comparing them with observational studies. Also, the limitations of the current modeling and future directions are discussed.

## 2 Model

The aim of the present study is to simulate circulation in Otsuchi Bay. Because the bay is open to the western boundary region of the North Pacific (Fig. 1) as mentioned above, appropriate conditions of the North Pacific are necessary for the bay simulation. In the present study, a “Pacific model” (hereafter, PM) and a “Bay model” (hereafter, BM) are constructed, and one-way nesting from PM to BM is performed.

## 2.1 Pacific model

PM is basically the same as Urakawa et al.'s (2015) triply nested grid OGCM. The model is a triply nested version of Kurogi et al.'s (2013) two-way nested grid OGCM, which was based on COCO (Hasumi 2006). The model domain of PM is different from Urakawa et al. (2015): PM covers the Pacific Ocean from 37.9°S to 67.68°N (Fig. 2), whereas Urakawa et al. (2015) covered from 15°S to 62°N. In the present study, tidal forcing is given as the tidal potential that is calculated from the orbital elements of the moon and the sun, whereas tidal forcing is not given in Urakawa et al.'s (2015) model.

Horizontal resolutions of outer, intermediate, and inner models of PM are  $0.5^\circ \times 0.5^\circ \cos \theta$ ,  $0.1^\circ \times 0.1^\circ \cos \theta$ , and  $0.02^\circ \times 0.02^\circ \cos \theta$ , respectively, where  $\theta$  is the latitude. Each model has 74 common vertical levels, in which the thickness is increasing from 5 m for the surface to 250 m for the deepest levels (9200-m depth).

Initial temperature and salinity distributions are given by climatology of the World Ocean Atlas 2009 (Locarnini et al. 2010; Antonov et al. 2010). The initial velocity field is a state of rest. From these initial conditions, the model is forced by Version 2 of the forcing of common ocean-ice reference experiment (CORE Ver. 2, Large and Yeager 2009) for 8 years. For more details, see Urakawa et al. (2015).

## 2.2 Bay model

BM is based on the triply nested grid OGCM (Urakawa et al. 2015). In order to realize one-way nesting from PM to BM, the model, which is constructed from outer, intermediate, and inner models, is modified as follows: the outer model of BM has the same horizontal grid spacing as the inner model of PM, and the communication between the outer and intermediate models of BM is one-way from the outer model to the intermediate one. The outer model is not actually calculated, but worked as a spatio-temporal interpolation unit of PM outputs, which are calculated in advance as mentioned above.

The model domain is shown in Fig. 2. Horizontal grid spacings of outer, intermediate, and inner models in BM are  $0.02^\circ \times 0.02^\circ \cos \theta$ ,  $0.0008^\circ \times 0.0008^\circ \cos \theta$ , and  $0.00016^\circ \times 0.00016^\circ \cos \theta$ . At the latitude where Otsuchi Bay is located ( $\sim 39.34^\circ\text{N}$ ), the latitudinal resolution is about 1720, 69, and 14 m, respectively. Each model has 50 common vertical levels. The vertical grid spacing is shown in Table 1.

The Smagorinsky type harmonic viscosity (Smagorinsky 1963) is applied for the lateral momentum mixing, whose control parameter is set to 0.4. Vertical eddy viscosity and diffusivity is determined by a turbulence closure

of Noh and Kim (1999). Horizontal and vertical advection schemes are UTOPIA (Leonard 1993, 1994) and QUICK-EST (Leonard 1979), respectively.

Over the shallow region in the bay, 2-m mesh topography observed after the disaster by side-scan sonars is available (T. Komatsu of AORI, personal communication). For the deeper region in the bay and outside the bay, Japan Ocean Data Center (JODC) Expert grid data for Geography (J-EGG500), which is a 500-m mesh topographic data set, and SRTM30\_PLUS (Becker et al. 2009), which is a 30-second mesh topographic data set, are used for BM. In order to avoid discrepancy between 2-m mesh data and 500-m or 30-s mesh data, the 2-m mesh data is first smoothed into 500-m mesh, then combined to 500-m or 30-s mesh data, and interpolated to the model grids by a spline interpolation. In order to determine coastlines, a 10-m elevation data set by Geospatial Information Authority of Japan (GSI, <http://www.gsi.go.jp/ENGLISH/index.html>) is used.

## 2.3 Boundary conditions for BM

In the present study, boundary conditions to BM are given by climatological ten-day averaged atmospheric forcing and river discharge. In order to make atmospheric forcing data that are imposed on BM, long-term data acquired via an observation station located to the south of ICRC (Fig. 1) are used. In the present study, ten-day averaged climatologies are made from 1998 to 2009 observations (Otobe et al. 1999, 2000, 2001, 2002, 2003, 2004, 2005, 2006; Sato et al. 2007, 2008; Michida et al. 2009, 2010) of 10-m wind, 2-m air temperature, 2-m relative humidity, downward shortwave flux, total downward radiative heat fluxes, evaporation, and sea surface pressure. Precipitation was observed only from 1998 to 2002, and its ten-day averaged climatology used in the present study is based on Otobe et al. (2003). In order to obtain surface wind stress, Large and Yeager's (2004) bulk formula is applied.

River discharge is also necessary for BM. For PM, a daily climatology of river discharge (Yoshimura et al. 2008) was given, and its ten-day-average was given at the coast of BM. There are three major rivers that flow into Otsuchi Bay from the western boundary of the bay (Kozuchi Riv., Otsuchi Riv., and Unosumai Riv., see Fig. 1), but they are not distinguished in PM. Anbo et al. (2005) summarized sporadic observations of the river discharge from 1974 to 2000, and they showed that their ratio (Kozuchi : Otsuchi : Unosumai) is 2:3:5 or 15:30:55, although the ratio varies from hour to hour, and season to season. In the present study, the ratio is fixed to 1:2:4. The river discharge given to Otsuchi Bay region in PM is divided into this ratio, and is given to BM by adding to precipitation at upstream areas of the three rivers.

**Fig. 2** Model domain and topography of **a** the outer model of PM, **b** the intermediate model of PM, **c** the inner model of PM, **d** the intermediate model of BM, and **e** the inner model of BM. Colors show the bottom topography (unit: m). Note that the color scales of PM (**a–c**) and BM (**d, e**) are different. The locations of *point A* and *lines* (L1, L2, L3, L3') are also shown in the figures that follow

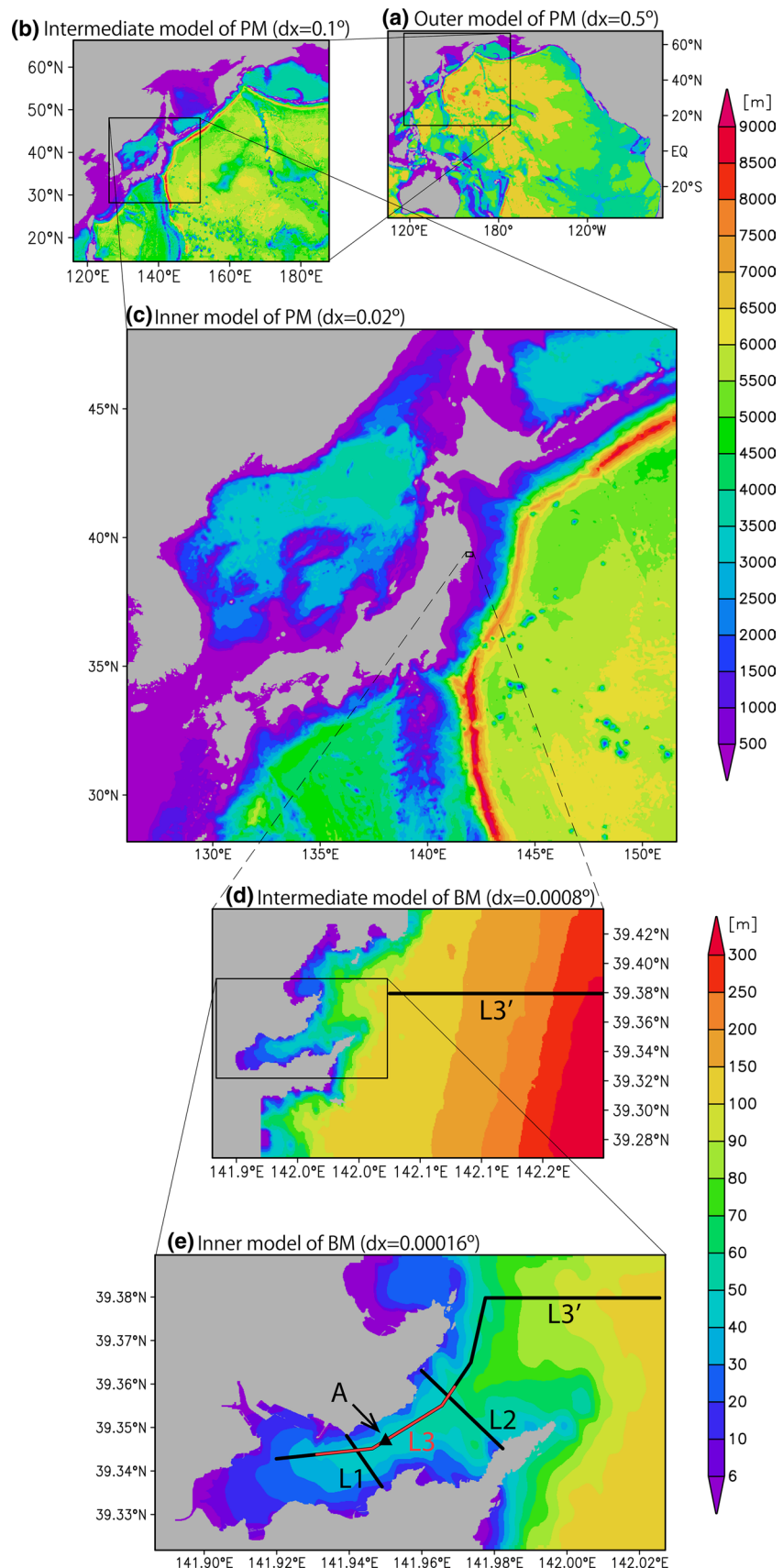


**Table 1** Vertical thickness ( $D_z$ ) of BM

| Layer number | $D_z$ (m) |
|--------------|-----------|
| 1            | 2.0       |
| 2–10         | 1.0       |
| 11–14        | 2.0       |
| 15–18        | 3.0       |
| 19–23        | 4.0       |
| 24–27        | 5.0       |
| 28–40        | 10.0      |
| 41–50        | 25.0      |

Note that the first layer is a  $\sigma$ -layer

Only in the area where river discharge is imposed, water temperature is relaxed to the value calculated from the sea surface temperature (SST) observed near the ICRC observational station. Although Anbo et al. (2005) reported that river water temperature is several degrees higher than SST in the bay in spring, and lower from autumn to winter, it is difficult to formulate the relationship between river water temperature and SST in the bay. In the present study, river water temperature is set to 3 K lower than the SST climatology, and the lower limit is set to 2 °C. The relaxation time constant is one day.

The outer model of BM works as a spatio-temporal interpolator of PM and realizes an off-line one-way nesting, as mentioned above. For the off-line inputs, hourly outputs of the seventh and eighth year of PM are used. As tidal forcing is given in the PM simulation, tides in BM are represented as results of one-way nesting from PM to BM.

## 2.4 Experiment

The initial condition of BM is a state of rest, with temperature and salinity fields adopted from the meridional mean at the first-hour-average (0:00–1:00) on November 1 of the seventh year of PM along the eastern boundary of BM. Spin-up of BM has two steps. First, wind and river discharge are given as zero at the initial state, and over the following 2 months, they are gradually increased to the values of November 1 of the seventh year of PM. During the first spin-up, there is no volume flux through the boundary from PM to BM, and accordingly, no tidal forcing is given. Second, over the following 2 weeks after the first 2-month spin-up, the volume fluxes through the boundary from PM to BM with tidal variability are gradually increased from zeros to the values of November 1 of the seventh year of PM. After the second spin-up, BM simulation is started from November 1 of the seventh year of PM to December 31 of the eighth year of PM. In the present study, the last one year forced by January 1 to December 31 of the eighth year of PM is presented.

In order to investigate intrusion processes of the Pacific water into Otsuchi Bay, a virtual tracer is also calculated online. Experiments with the virtual tracer begin on the first day of each month. The initial tracer values in BM are zero, and the tracer values are kept at unity at the open boundary during the experiments.

## 3 Results

In this section, results of the inner model of BM are described. First, monthly mean circulations in Otsuchi Bay are shown in Section 3.1. Next, intrusion processes of the Pacific water in winter and summer are presented by results of the virtual tracer experiments in Section 3.2. Finally, seasonality of baroclinicity in the bay inferred by the virtual tracer experiment is discussed in Section 3.3.

### 3.1 Seasonal variation of monthly mean circulation in Otsuchi Bay

In winter (January, February, and December), the surface current at the bay mouth is with inflow almost everywhere, and the inflowing warmer and more saline water intrudes along the northern coast of the bay (Fig. 3a for January, and Suppl. Figs. S2 and S12 for February and December, respectively). Fresher and colder water in the inner part of the bay, which is influenced by the river discharge, is confined near the southern coast of the bay and is outflowing along the southern coast. In the western part of the bay, these flows form an anticlockwise circulation. On the other hand, the waters from the bay mouth and rivers are mixed in the middle part of the bay and flow out in the bottom layer of the bay mouth (Fig. 3a, Suppl. Figs. S2 and S12). Along L1, vertical distributions of salinity in January (Fig. 4a) and February (Suppl. Fig. S14) show a weak stratification caused by the river water, and it is well mixed in December (Supplementary Fig. S24). At the bay mouth (along L2), it is also well mixed vertically (Suppl. Fig. S24).

From spring to autumn (from March to October), the increased river water causes strong stratification and makes a pycnocline in the upper 10-m (Fig. 4b for August, and Suppl. Figs. S15–S22 for March to October). In the surface layer above the pycnocline, the water is outflowing almost everywhere, and an anticlockwise circulation is dominant below the pycnocline that saline water coming from the Pacific Ocean occupies (Figs. 3b, 4b, Suppl. Figs. S3–S10, and S15–S22). The surface outflow and the inflow below the pycnocline in the northern part of the bay are intensified from July to September (Fig. 4b and Suppl. Figs. S19–21). This is likely to be caused by an intensification of an estuary circulation driven by the river water discharge, but it is not clear

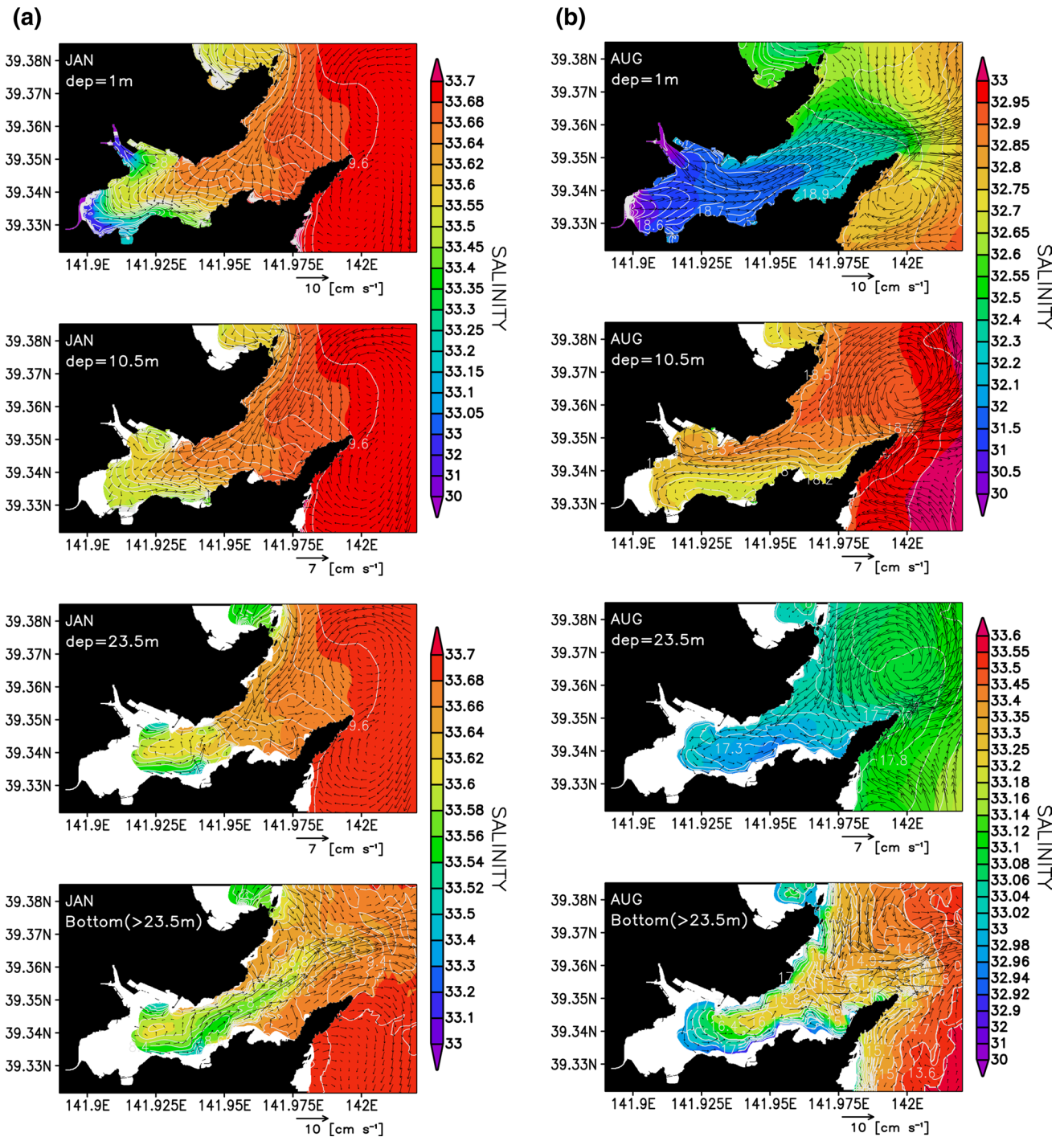


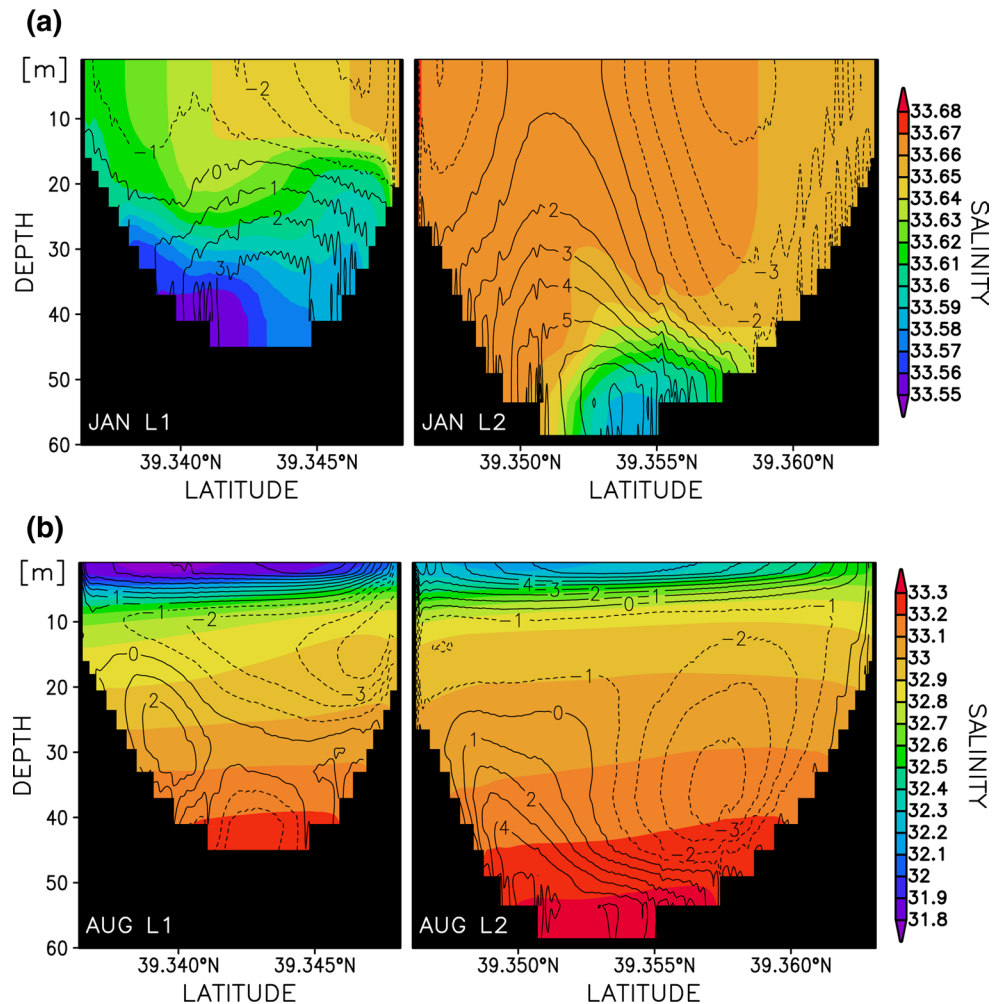
**Fig. 3** **a** Monthly mean salinity (colors, practical salinity unit), temperature (contours, unit: °C, contour interval: 0.1 °C) and current velocity (vectors, unit: cm s<sup>-1</sup>) in January. From top to bottom, the monthly means at the surface, at 10.5-m depth, at 23.5-m depth and at the sea bottom deeper than 23.5-m depth are shown. Note that the

vector scales are denoted below each panel, and the vectors are drawn on every 20th grid point in both the *x* and *y* direction. Also note that the salinity color scales of the upper two panels are different from the lower two panels. **b** Same as for **a**, but for August

because the transport of the Tsugaru Warm Current is also intensified during these seasons (Conlon 1982; Yasuda et al. 1988), and it has potential to influence the intensification of the inflow.

The stratification in these seasons is strong, so that the water below the pycnocline is weakly mixed with the river water in the inner part of the bay, and the fresher water causes a meridional salinity gradient through the

**Fig. 4** **a** Monthly mean salinity (colors, practical salinity unit) and cross-sectional component of velocity (contours, unit:  $\text{cm s}^{-1}$ , contour interval:  $1 \text{ cm s}^{-1}$ ) along L1 (left panel) and L2 (right panel) in January. Positive and negative values indicate offshore and onshore directions normal to each section, respectively. See Fig. 2e for the locations of L1 and L2. **b** Same as the **a**, but for August



anticlockwise circulation, which advects the fresher water in the southern part of the bay (Fig. 4b). Such a salinity contrast is also found by an observational study (Ishizuka et al. unpublished). Related to this salinity gradient, the depth of outflowing core along the southern coast is deeper than the depth of the inflowing core along the northern coast by about 10 m. This difference of the core depths between the northern inflow and the southern outflow is clear by observational studies (Otobe et al. 2009).

### 3.2 Pacific water intrusion

The Pacific water has an impact on the water environment in Otsuchi Bay as shown in the Section 3.1. In Fig. 5, temporal successions of the virtual tracer originated by the North Pacific in January and August are shown as the typical cases of winter and summer, respectively.

In January, the tracer is intruding into the bay almost in phase, except for the bottom layer (Fig. 5a) because the upper layer water, which has 20-m thickness or more, is flowing in (Figs. 3a, 4a). Beneath the upper layer, on the other hand, an

outflow prevails and is not in phase with the upper layer. This can also be seen in Fig. 6a, which is a vertical-temporal diagram at point A (see Fig. 2 for its location). The tracer concentration in the upper 20-m depth is increasing in phase and lags beneath the upper layer. In the inner part of the bay, the concentration of the Pacific water is relatively low, because there is river water discharge in this region (Fig. 3a).

In August, the Pacific water intrudes into the bay below the pycnocline (Fig. 5b), above which a low salinity water outflow exists (Figs. 3b, 4b). It is not clear whether the intrusion below the pycnocline is in phase or not in Fig. 5b. A vertical-temporal diagram at point A shows that there are two centers of the Pacific water intrusion between 10-m and 20-m depths, and deeper than 30-m depth (Fig. 6b). Also, the tracer concentration increases with oscillations, which are out of phase between the two cores. Time series of the tracer concentration at 16-m and 41-m depths, and their anomalies from 49-h window clearly show the out of phase variabilities between these two depths (Fig. 6c, d). This implies the existence of baroclinic tides in Otsuchi Bay during summer.

### 3.3 Seasonality of baroclinicity

In order to show a time variation of baroclinicity in the bay, time series of correlations among zonal velocities at 16-m (upper subsurface) and 41-m depths (near bottom) and zonal barotropic velocity at point A are presented in Fig. 7. Note that the four major tidal components (K1, O1, M2, and S2) are removed from zonal velocities at 16-m and 41-m depths by a harmonic analysis in order to eliminate oscillating motion by tides. From late April to September, the bottom layer velocity is in phase with the barotropic motion (red line in Fig. 7). In the upper subsurface layer, on the other hand, the velocity is almost out of phase with bottom layer and barotropic velocities during the same season, especially from July to September (the black line in Fig. 7). The baroclinicity also can be seen in the monthly mean velocity along L1 in July (Suppl. Fig. S19) and August (Fig. 4b).

How is the variability of the baroclinicity in diurnal time scales? The bottom layer velocity and its normalized product with the upper subsurface velocity in August are plotted in Fig. 8. A negative value of the latter means that the direction of the upper subsurface and bottom layer flows is opposite, which means a baroclinicity. As the bottom layer is in phase with the barotropic velocity (the red line in Fig. 7), Fig. 8 clearly shows that the baroclinicity is enhanced while the barotropic motion is featured as both flood and ebb tides (Fig. 8). For example, baroclinic tides from August 16 to 17 are illustrated in Fig. 9. The baroclinic tides always emerges with the phase variation associated with the barotropic tidal motion.

These results imply a relationship between observational intermittent detections of Tsugaru Warm Current Water at the bottom layer of the bay during summer or early autumn in Otsuchi Bay and baroclinic tides. A similar detection during October 1984 in Toni Bay, which is about 15 km south of Otsuchi Bay, was also reported (Okazaki et al. 1994). This is discussed in the next session.

## 4 Summary and discussion

A numerical simulation was performed to investigate the circulation in Otsuchi Bay, and a seasonal variability in the mean circulation was obtained. Basic circulation is an anticyclonic circulation, composed of an inflow along the northern coast and an outflow along the southern coast. In winter, the circulation in the eastern part of the bay is altered to an inflow in the upper layer and outflow in the bottom layer. From spring to autumn, the surface light water originating in the river discharge caps the anticyclonic circulation and forms an outflow.

**Fig. 5** **a** Concentration of the Pacific water tracer from January 6 (top panels) to 14 (bottom panels). Hourly means from 0:00 to 1:00 of each day at the surface (left panels), 10.5-m depth (second panels from the left), 23.5-m depth (second panels from right) and the bottom deeper than 23.5-m depth (right panels) are shown. The values shown by colors are non-dimensional. **b** Same as **a**, but for August

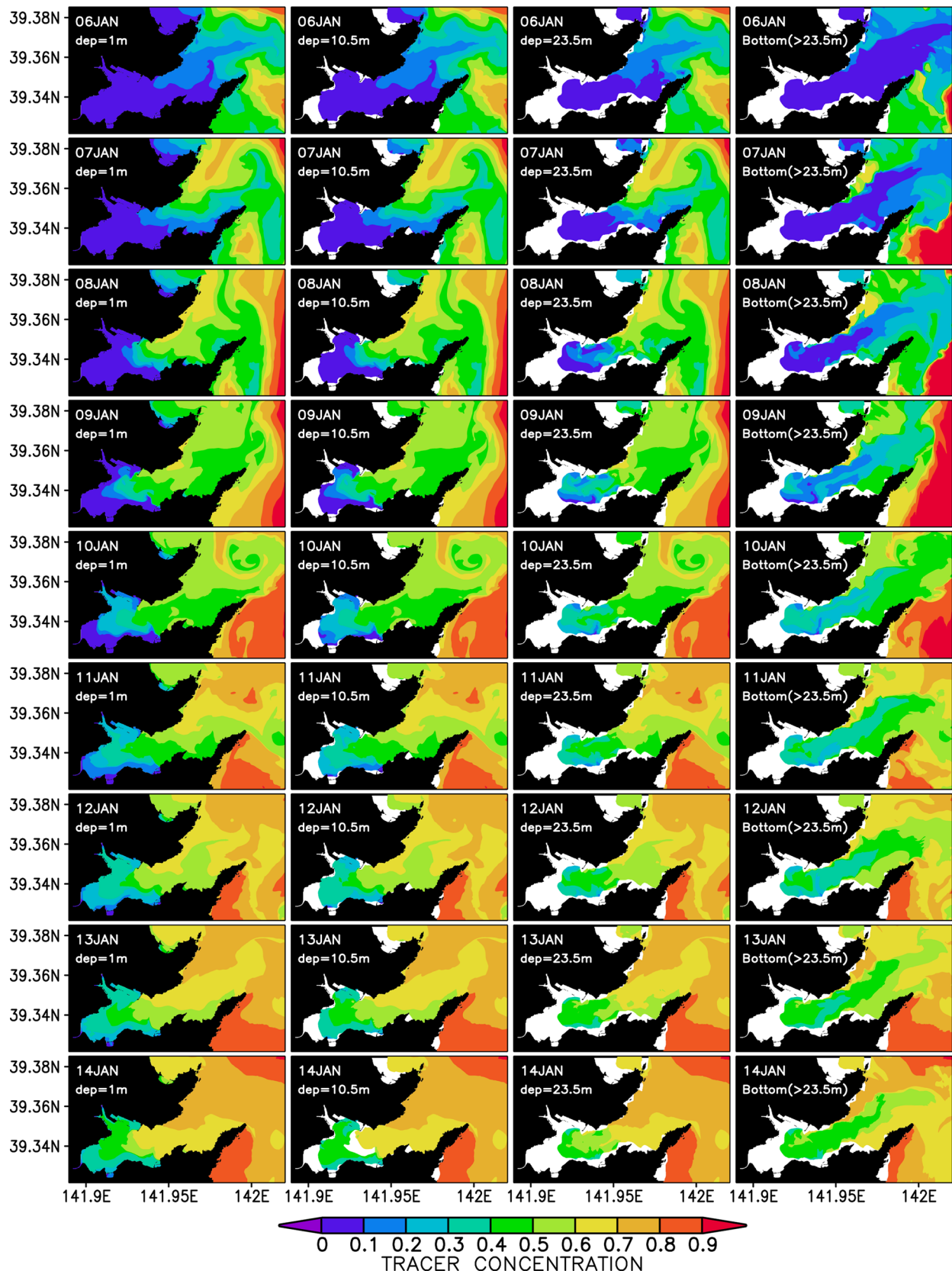
The process of the Pacific water intrusion into the bay depends not only on the mean anticyclonic circulation, but also the stratification and tides. The appearance of baroclinic tides in the bay from spring to autumn is a key role of the water exchange between the bay and the North Pacific Ocean.

The mean anticyclonic circulation in Otsuchi Bay from spring to autumn is qualitatively consistent with an observational discussion by Otobe et al. (2009). Quantitatively, the velocity of the anticyclonic circulation in the present simulation, whose maximum is  $\sim 4 \text{ cm s}^{-1}$ , is consistent with the observations that reported the maximum velocity as  $\sim 5 \text{ cm s}^{-1}$ . This circulation is likely to be influenced by the Coriolis force. The internal Rossby radius of deformation estimated the averaged density along the L1 in the model; it was 1–2 km with seasonal variation. Since the width of Otsuchi Bay is about 2 km as described above, it is inferred that the anticyclonic circulation in the bay is formed by a balance between the Coriolis force and the pressure gradient.

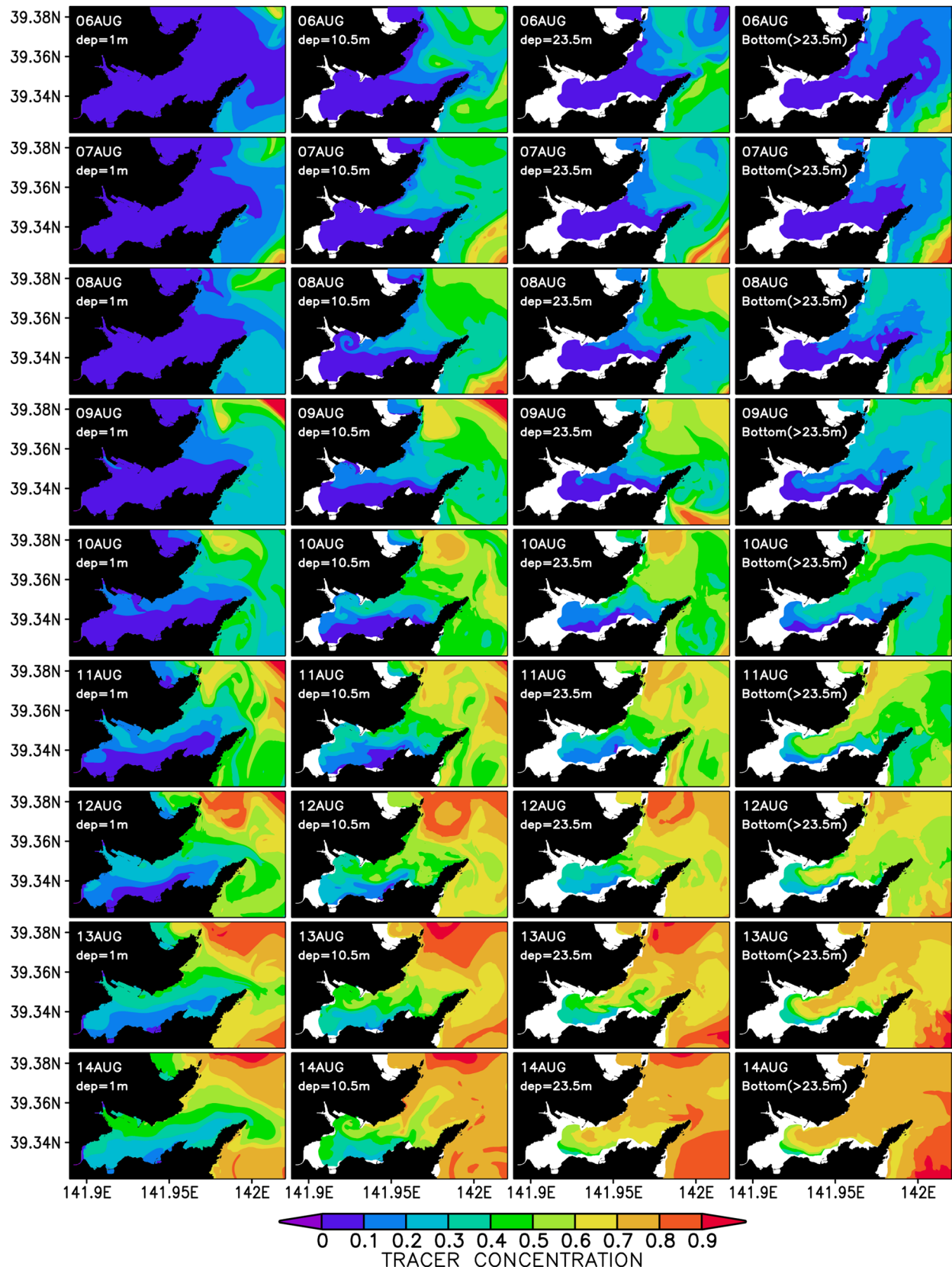
The intensification of circulation during summer (Suppl. Figs. S19–S21) is also consistent with the observational study (Ishizu et al. unpublished). However, the surface intense outflow seen from spring to autumn in the present study cannot be found in their observations. Because they use bottom moored ADCPs that cannot capture the surface current above about 9-m depth, we cannot judge whether the surface outflow in the present model really exists or not. Meanwhile, Tanaka et al. (2015) found surface low salinity waters in the bay during summer, and they inferred that the surface low salinity waters are from the rivers.

In winter, the mean circulation does not coincide with the observations. We speculate that the winter circulation in the bay varies from year to year and from month to month. Otobe et al. (2009) reported that the dominant circulation during the winter 2003–2004 is an estuary-like circulation composed of a surface outflow and compensating inflow in deeper water in the bay. On the other hand, Ishizu et al. (unpublished) showed that an anticyclonic circulation is dominant from January to February 2013. They also showed an inflow in the upper layer and an outflow in bottom layer in January 2014, and a clockwise circulation in February 2014. The variability of the dominant circulation in winter is partly influenced by the condition in the North Pacific off the Otsuchi Bay. Compiling and analyzing the

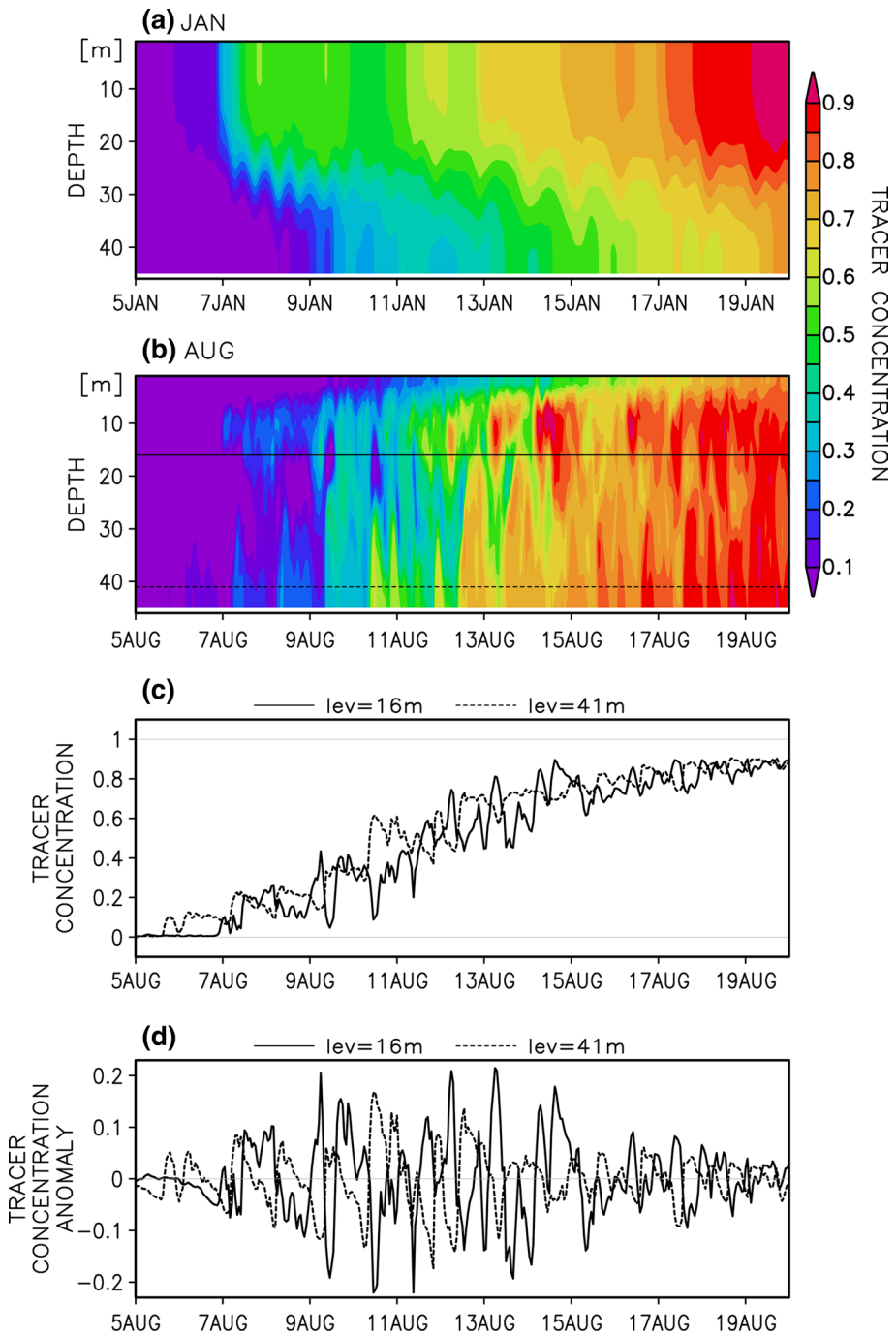
(a)



(b)

**Fig. 5** continued

**Fig. 6** **a** Concentration of the Pacific water tracer at the point A located at 39.347°N, 141.95°E (Fig. 2e) from January 5 to 20. **b** Same as **a**, but for August 5 to 20. **c** Same as **b**, but at 16-m depth (*solid line*) and 41-m depth (*dashed line*). Corresponding depths are shown in **b** as *solid* and *dashed lines*, respectively. **d** Same as **c**, but for the anomalies from 49-h window averages



observational evidences and model simulations is one of our future works.

The occurrence of the baroclinic tidal flow from spring to autumn is possibly related to the seasonal stratification variability. In winter, the thickness of the surface mixed layer becomes larger than in other seasons, and baroclinicity in the bay is weak. On the other hand, during spring to autumn, even the water beneath the sharp pycnocline in the bay is stratified (Fig. 4b). The mixed layer depth in the open ocean becomes

shallower during these seasons, too (figures not shown). The shoaled pycnocline in the Pacific may influence the baroclinic tides in the bay. Indeed, water temperature at a point located at the middle part of the bay (point A) shows larger amplitude of high frequency oscillation (Fig. 10a). This oscillation has diurnal/semidiurnal periods, and this seems to be propagated from the shelf break region (Fig. 10b). In addition, it is possible that coastal Kelvin waves, which are generated by the diurnal/semidiurnal tides to the north of Otsuchi Bay,

**Fig. 7** Correlations between the zonal barotropic velocity and the zonal velocity at 16-m depth (black line), the zonal barotropic velocity and the zonal velocity at 41-m depth (red line), and the zonal velocities at 16-m and 41-m depths at point A (Fig. 2e). The correlations are calculated by using anomalies from 49-h window averages. Note that the four major tidal components ( $K_1$ ,  $O_1$ ,  $M_2$ , and  $S_2$ ) are removed from the zonal velocities at 16-m and 41-m depths by a harmonic analysis

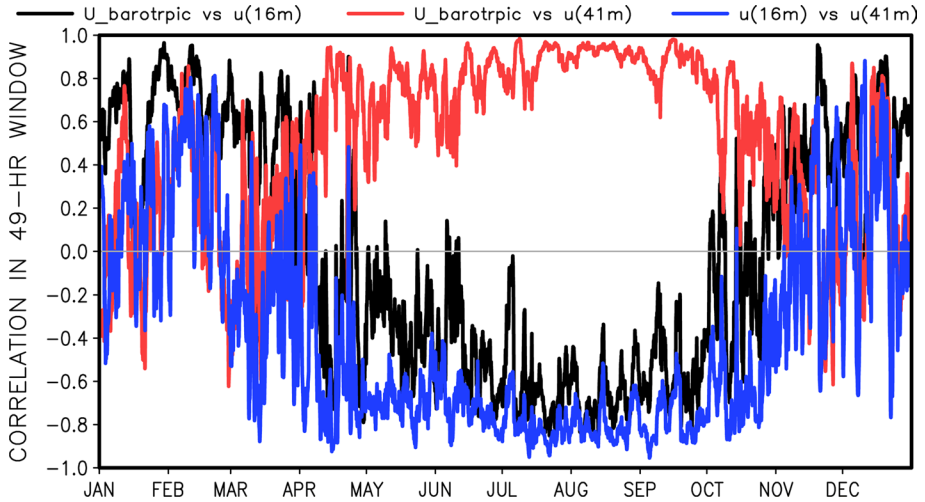
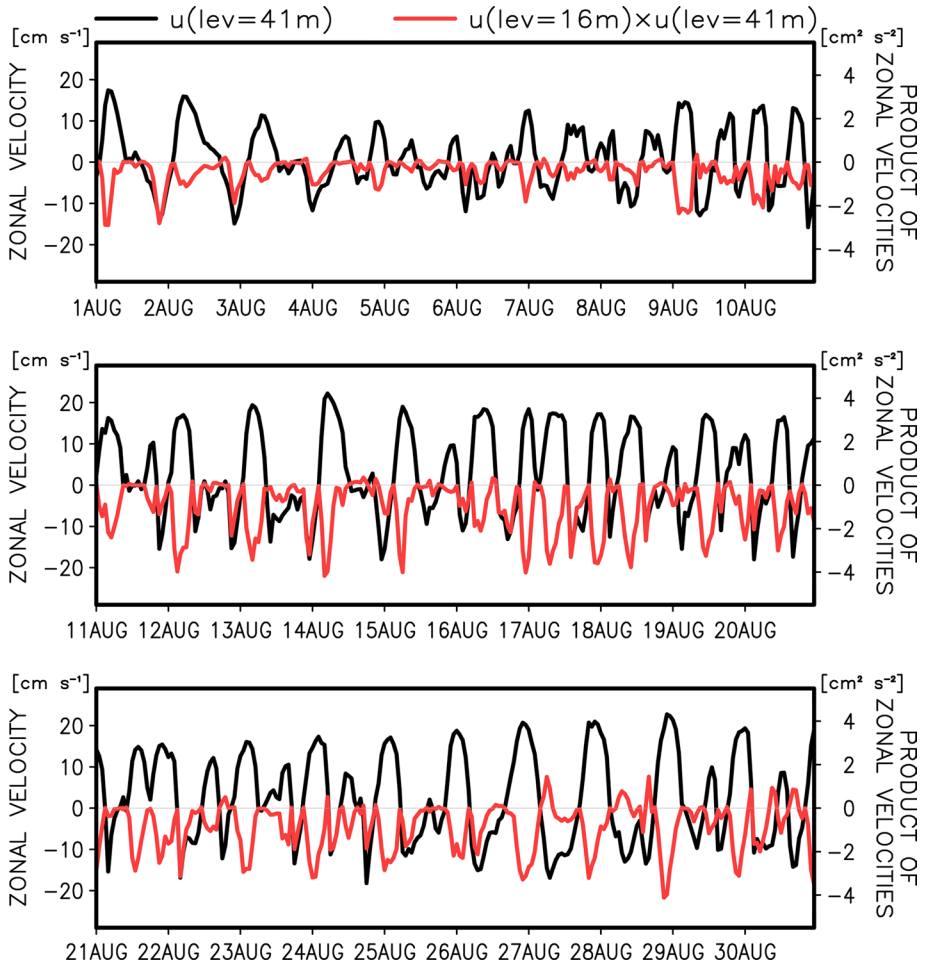


**Fig. 8** Time series of the zonal velocity at 41-m depth (black line, unit:  $\text{cm s}^{-1}$ ) and a product of the zonal velocities at 16-m and 41-depths (red line, unit:  $\text{cm}^2 \text{s}^{-2}$ ) during August at point A (Fig. 2e). The products shown by red lines are normalized by the standard deviation from their average during the designated period. The four major tidal components are removed from the velocities



propagate to the bay and influence the short time variability. Although it is not clarified that the baroclinic tide in Otsuchi Bay detected in the model is caused by interface oscillations with the barotropic tide, propagations of the internal tide, or propagations of coastal Kelvin

waves, it is an interesting topic to address the variability in the bay. Tanaka et al. (2015) shows that the baroclinic tide in Otsuchi Bay was observed in summer. The mechanism of the baroclinic tide in the bay will be revealed by observational and numerical studies.

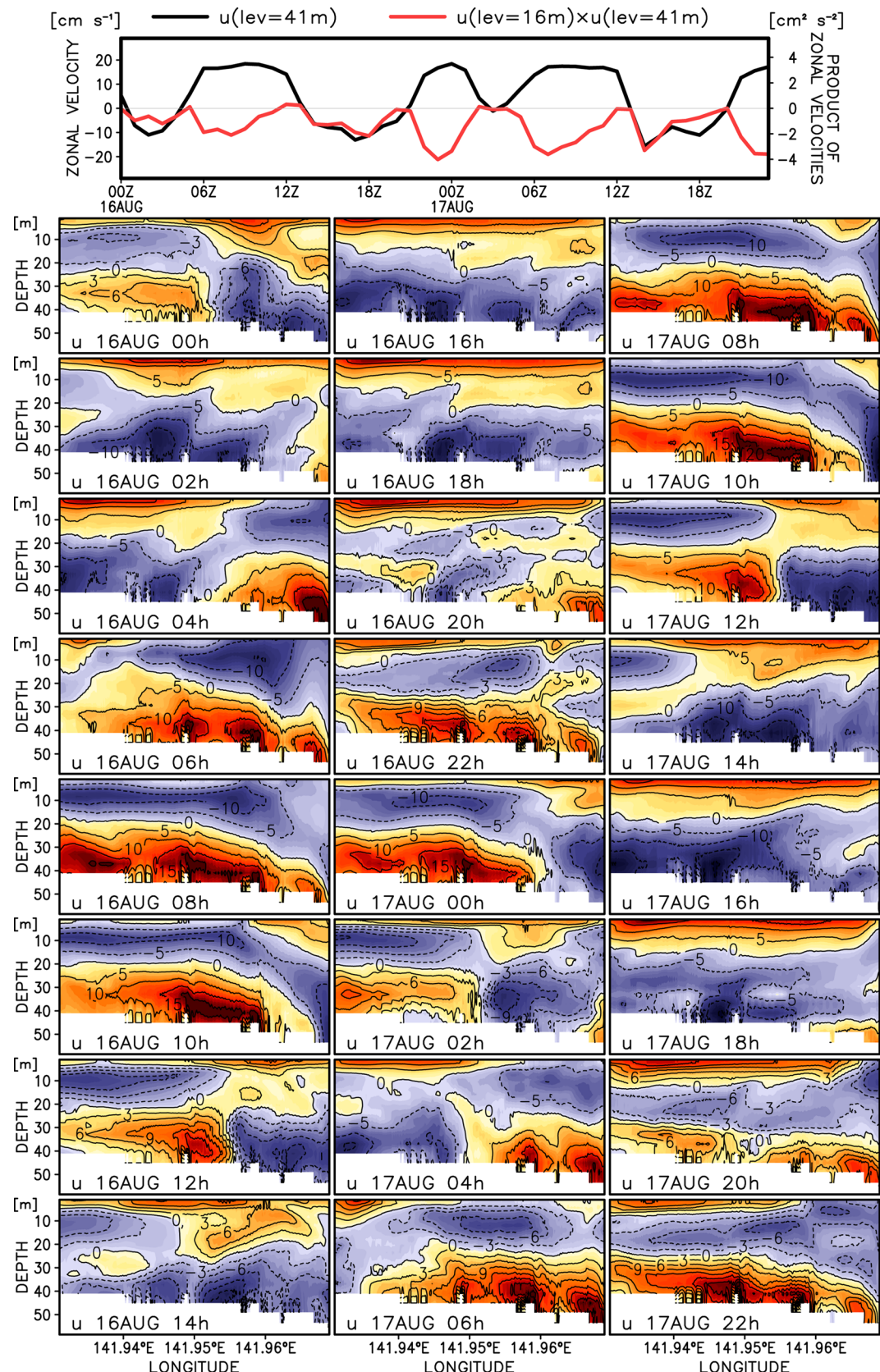
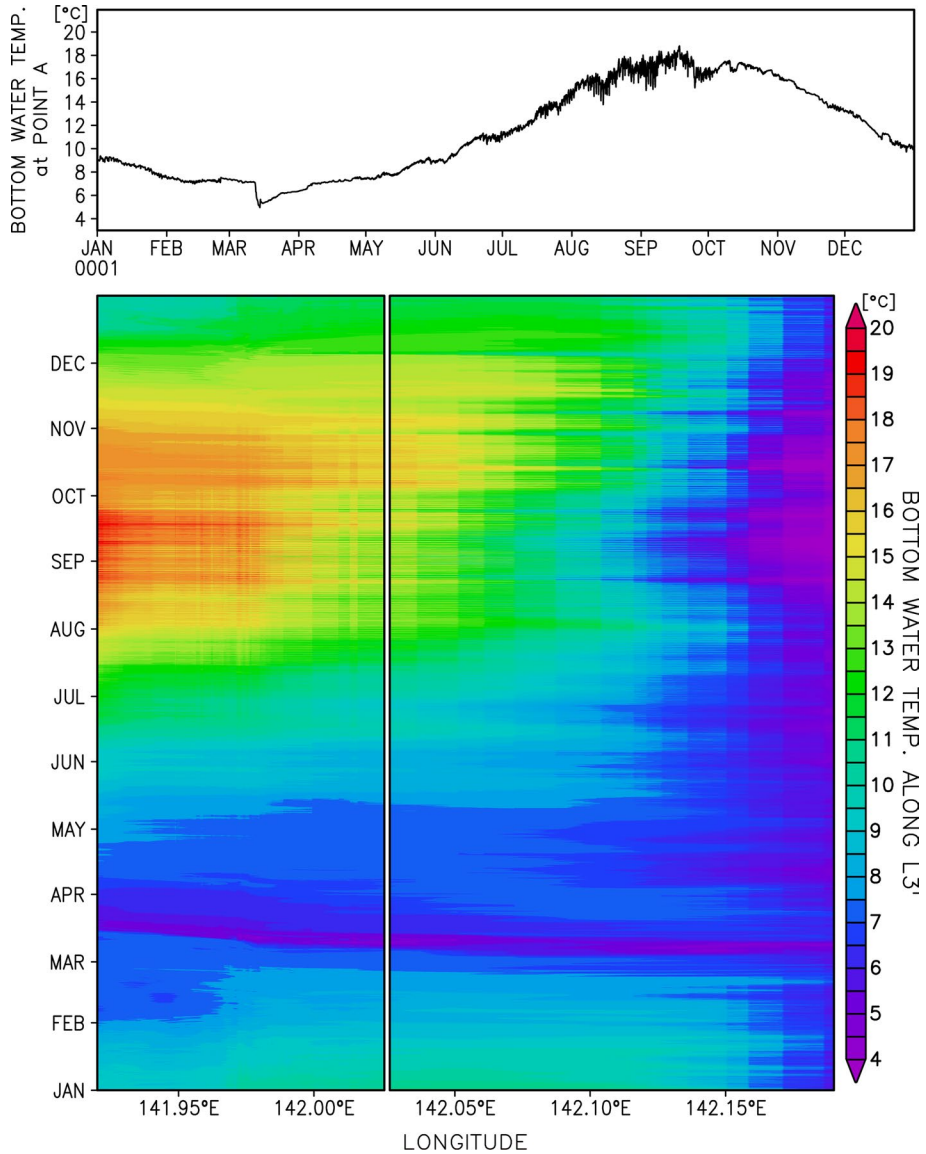


**Fig. 9** (Upper panel) same as Fig. 8, but for the period from August 16 to 17. (Lower panels) Hourly mean zonal velocity along the line L3 (Fig. 2e). Unit of the lower panels is cm s<sup>-1</sup>. The four major tidal components are also removed from the velocities shown in the lower panel

**Fig. 10** Temperature just above the sea bottom (unit: °C). The *Upper panel* shows the bottom temperature at point A (Fig. 2e), and the *lower panel* shows it along the line L3' (Fig. 2d, e). Note that the lower panel is divided into the outputs from the inner model (*left*) and the intermediate model (*right*) of BM

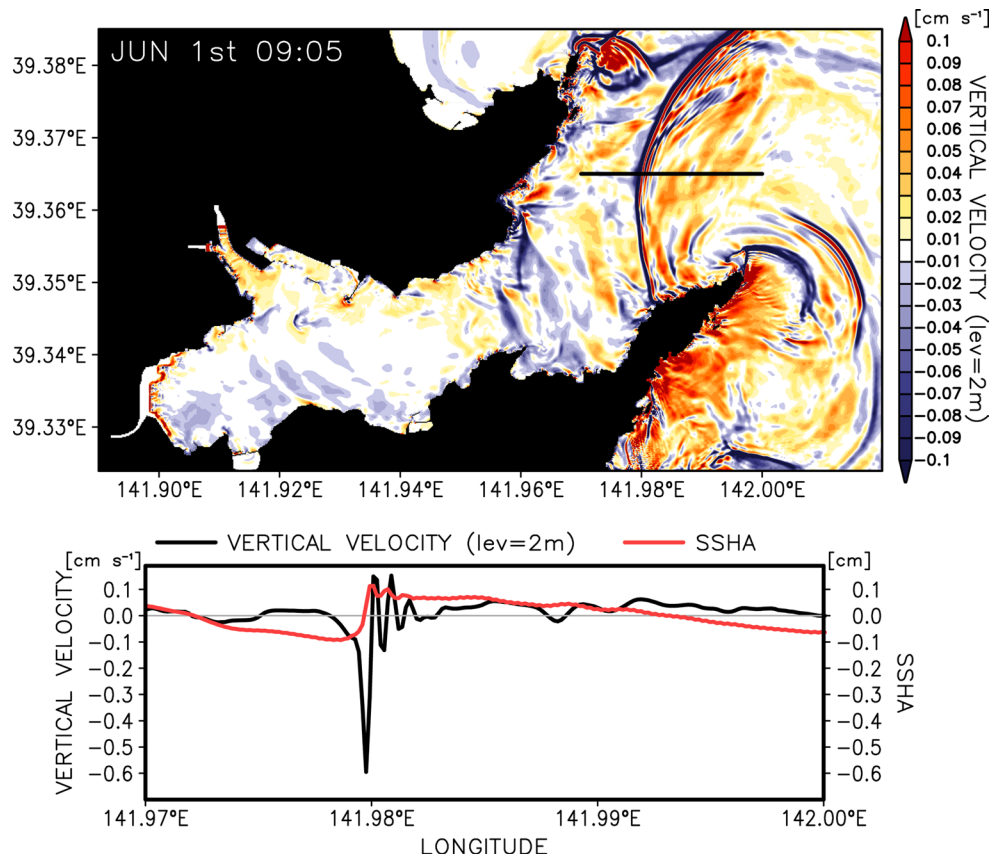


Although the horizontal resolution of the model used here is fine, some features of mean circulation in the bay obtained by observations, for example, in winter, are different. Of course, there are some uncertainties in numerical models, and one of them is caused by the boundary conditions. The target of the present study is a climatological mean and seasonal variability of the circulation in the bay. In contrast, an observed example represents a specific time or period. In order to resolve the gap between observations and model results, continuous long-term observations are necessary. In the present study, the source of diurnal variation is assigned to tides, but a variability of wind, for example, land and sea breeze in spring to autumn, may also be a source of it. In addition, wind forcing observed at a station is applied to the present model. Actually, wind over the bay must be influenced by the topography around Otsuchi Bay. The problem of temporal resolution of wind forcing will

be resolved by a successive observation (Komatsu et al. unpublished). A numerical simulation by an atmospheric model is a candidate to resolve the problem. Also, it is possible that a horizontal resolution gap between BM and PM (25 times larger in PM than in BM) causes some problems. The authors are planning to perform a PM simulation with finer resolution, which reduces the gap to five times larger in PM than in BM, and we are expecting to improve the BM simulation.

In order to simulate turbulence of O (10 m) for the horizontal scale and O (1 m) for the vertical scale, which is comparable to the inner model of BM, a non-hydrostatic model is usually employed. Even the model used in the present study, which is hydrostatic, represents “bore-like” phenomena. In Fig. 11, it is captured as a jump of vertical motion across a tidal front and sequential waves behind the front, even though the tidal front is expressed as several millimeters by

**Fig. 11** (Upper) a snapshot of vertical velocity on June 1, 09:05, at 2-m depth (colors, unit:  $\text{cm s}^{-1}$ ). (Lower) the snapshots of the vertical velocity at 2-m depth and sea surface height anomaly (SSHA) along the thick black line shown in the upper panel



the sea surface height. However, a hydrostatic model cannot represent some mixing processes, such as wave breakings, which are possibly induced after tidal bores are approaching a shallow coastal region. In order to know whether such processes play a key role or not in the circulation of Otsuchi Bay, a non-hydrostatic simulation is essential. A non-hydrostatic modeling of the bay will be the next step in our study.

Our next goal is constructing a marine ecosystem model in Otsuchi Bay. As shown by the present study, the Pacific water plays an important role in the exchanging mechanism of seawater in the bay. It is expected that the water exchange process largely influences the mechanisms of the ecosystem in the bay, and the results of the present study will make it possible to make quantitative estimates.

**Acknowledgments** This work is supported by a project named ‘Tohoku Ecosystem-Associated Marine Sciences’, which is produced by the Ministry of Education, Culture, Sports, Science and Technology of Japan. The authors also appreciate Dr. Masao Kurogi of Japan Agency for Marine-Earth Science and Technology (JAMSTEC) for his advice to develop the nested-grid ocean model.

## References

- Anbo A, Otobe H, Takagi M (2005) On the river water discharged into Otsuchi Bay. Rep Int Coast Res Center 30:4–8 (in Japanese)
- Antonov JI, Seidov D, Boyer TP, Locarnini RA, Mishonov AV, Garcia HE, Baranova OK, Zweng MM, Johnson DR (2010) World Ocean Atlas 2009, Volume 2: Salinity. S. Levitus, Ed. NOAA Atlas NESDIS 69, US Government Printing Office, Washington, DC
- Becker JJ, Sandwell DT, Smith WHF, Braud J, Binder B, Depner J, Fabre D, Factor J, Ingalls S, Kim SH, Ladner R, Marks K, Nelson S, Pharaoh A, Trimmer R, Von Rosenberg J, Wallace G, Weatherall P (2009) Global bathymetry and elevation data at 30 arc seconds resolution: SRTM30\_PLUS. Mar Geodesy 32:355–371
- Conlon DM (1982) On the outflow modes of the Tsugaru Warm Current. La Mer 20:60–64
- Fukuda H, Katayama R, Yang Y, Takasu H, Nishibe Y, Tsuda A, Nagata T (2015) Nutrient status of Otsuchi Bay (northeastern Japan) following the 2011 off the Pacific coast of Tohoku Earthquake. J Oceanogr. doi:[10.1007/s10872-015-0296-2](https://doi.org/10.1007/s10872-015-0296-2)
- Hasumi H (2006) CCSR Ocean Component Model (COCO) version 4.0. CCSR Report 25, Center for Climate System Research, University of Tokyo
- Kawamiya M, Kishi MJ, Kawser Ahmed MD, Sugimoto T (1996) Causes and consequences of spring phytoplankton blooms in Otsuchi Bay, Japan. Cont Shelf Res 16:1683–1698
- Noh Y, Kim, HJ (1999) Simulations of temperature and turbulence structure of the oceanic boundary layer with the improved near-surface process. Journal of Geophysical Research 104(C7):15,621–634 doi:[10.1029/1999JC900068](https://doi.org/10.1029/1999JC900068)
- Kishi M, Higashi N, Takagi M, Sekiguchi K, Otobe H, Furuya K, Aiki T (2003) Effect of aquaculture on material cycles in Otsuchi Bay, Japan. Otsuchi Mar Sci 28:65–71
- Kurogi M, Hasumi H, Tanaka Y (2013) Effects of stretching on main-tain the Kuroshio meander. J Geophys Res 118:1182–1194. doi:[10.1002/jgrc.2012](https://doi.org/10.1002/jgrc.2012)

- Large WG, Yeager SG (2004) Diurnal to decadal global forcing for ocean and seaice models: the data sets and climatologies. NCAR Technical Report TN-460 + STR, National Center for Atmospheric Research
- Large WG, Yeager SG (2009) The global climatology of an inter-annually varying air-sea flux data set. *Clim Dyn* 33:341–364. doi:[10.1007/s00382-008-0441-3](https://doi.org/10.1007/s00382-008-0441-3)
- Leonard BP (1979) A stable and accurate convective modeling procedure based on quadratic upstream interpolation. *Comput Methods Appl Mech Eng* 19:59–98
- Leonard, BP, MacVean MK, Lock AP (1993) Positivity-preserving numerical schemes for multidimensional convection and diffusion. NASA Technical Memorandum 106055, ICOMP-93-05
- Leonard BP, MacVean MK, Lock AP (1994) The flux-integra method for multidimensional convection and diffusion. NASA Technical Memorandum 106679, ICOMP-94-13
- Locarnini RA, Mishonov AV, Antonov JI, Boyer TP, Garcia HE, Baranova OK, Zweng MM, Johnson DR (2010) World Ocean Atlas 2009, Volume 1: Temperature. S. Levitus, Ed. NOAA Atlas NESDIS 68, US Government Printing Office, Washington, DC
- Michida Y, Sato K, Otsuki M, Kurosawa M, Morita K, Takada J, Yamazaki T (2009) Results of oceanographic and meteorological observation in Otsuchi Bay. *Rep Otsuchi Mar Res Cent* 34:31–43 (in Japanese)
- Michida Y, Sato K, Otsuki M, Kurosawa M, Morita K, Hirano M, Yamazaki T (2010) Results of oceanographic and meteorological observation in Otsuchi Bay. *Rep Otsuchi Mar Res Cent* 35:57–63 (in Japanese)
- Nishibe Y, Isami H, Fukuda H, Nishida S, Nagata T, Tachibana A, Tsuda A (2015) Impact of the 2011 Tohoku earthquake tsunami on zooplankton community in Otsuchi Bay, northeastern Japan. *J Oceanogr*. doi: [10.1007/s10872-015-0339-8](https://doi.org/10.1007/s10872-015-0339-8)
- Okazaki M (1994) The circulation of sea water and the variation of the properties in some bays of Sanriku Coast, eastern coast of northern Japan. *Bull Coast Oceanogr* 32:15–28 (in Japanese)
- Otobe H, Shikama N, Nakai S, Taira K, Hattori A (1979) Preliminary observation on heat budget across the sea surface in Otsuchi Bay. *Rep Otsuchi Mar Res Cent* 5:1–7
- Otobe H, Takeuchi I, Konashi S (1996) Water flow structure near the Nanamodori point in Otsuchi Bay. *Otsuchi Mar Res Cent Rep* 21:51–58 (in Japanese)
- Otobe H, Otsuki M, Morita K, Kurosawa M, Iwama Y, Kashiwazaki K (1999) Results of oceanographic and meteorological observation in Otsuchi Bay. *Otsuchi Mar Sci* 24:58–72 (in Japanese)
- Otobe H, Otsuki M, Morita K, Kurosawa M, Iwama Y, Kashiwazaki K, Kurosawa M (2000) Results of oceanographic and meteorological observation in Otsuchi Bay. *Otsuchi Mar Sci* 25:78–89 (in Japanese)
- Otobe H, Otsuki M, Morita K, Kurosawa M, Iwama Y (2001) Results of oceanographic and meteorological observation in Otsuchi Bay. *Otsuchi Mar Sci* 26:107–121 (in Japanese)
- Otobe H, Otsuki M, Morita K, Kurosawa M, Iwama Y, Shodoshima K (2002) Results of oceanographic and meteorological observation in Otsuchi Bay. *Otsuchi Mar Sci* 27:86–100 (in Japanese)
- Otobe H, Otsuki M, Morita K, Kurosawa M, Kurosawa M, Iwama Y, Shodoshima K (2003) Results of oceanographic and meteorological observation in Otsuchi Bay. *Rep Otsuchi Mar Res Cent* 28:29–41 (in Japanese)
- Otobe H, Otsuki M, Morita K, Kurosawa M, Shodoshima K (2004) Results of oceanographic and meteorological observation in Otsuchi Bay. *Rep Int Mar Res Cent* 29:34–45 (in Japanese)
- Otobe H, Otsuki M, Morita K, Kurosawa M, Shodoshima K (2005) Results of oceanographic and meteorological observation in Otsuchi Bay. *Rep Otsuchi Mar Res Cent* 30:51–62 (in Japanese)
- Otobe H, Otsuki M, Morita K, Kurosawa M, Shodoshima K, Takada J (2006) Results of oceanographic and meteorological observation in Otsuchi Bay. *Rep Otsuchi Mar Res Cent* 31:40–51 (in Japanese)
- Otobe H, Onishi H, Inada M, Michida Y, Terazaki M (2009) Estimation of water circulation in Otsuchi Bay, Japan inferred from ADCP observation. *Coast Mar Sci* 33:78–86
- Sato K, Otsuki M, Morita K, Kurosawa M, Takada J (2007) Results of oceanographic and meteorological observation in Otsuchi Bay. *Rep Otsuchi Mar Res Cent* 32:37–47 (in Japanese)
- Sato K, Michida Y, Otsuki M, Morita K, Kurosawa M, Takada J (2008) Results of oceanographic and meteorological observation in Otsuchi Bay. *Rep Otsuchi Mar Res Cent* 33:43–54 (in Japanese)
- Smagorinsky J (1963) General circulation experiments with the primitive equations. *Mon Weather Rev* 91:99–164
- Tanaka K, Komatsu K, Itoh S, Yanagimoto D, Ishizu M, Hasumi H, Sakamoto TT, Urakawa SL, Michida Y, Saito K (2015) Baroclinic circulation and its variability in Otsuchi Bay on Sanriku ria coast. *J Oceanogr*. doi: [10.1007/s10872-015-0338-9](https://doi.org/10.1007/s10872-015-0338-9)
- Urakawa SL, Yoshimura K, Hasumi H (2015) Modeling low salinity waters along the coast around Japan using a high-resolution river discharge dataset. *J Oceanogr* 71:715–739. doi: [10.1007/s10872-015-0314-4](https://doi.org/10.1007/s10872-015-0314-4)
- Yasuda I, Okuda K, Hirai M, Ogawa Y, Kudoh H, Fukushima S, Mizuno K (1988) Short-term variations of the Tsugaru Warm Current in Autumn. *Bull Tohoku Reg Fish Res Lab* 50:153–191 (in Japanese)
- Yoshimura K, Sakimura T, Oki T, Kanae S, Seto S (2008) Toward flood risk prediction: a statistical approach using a 29-year river discharge simulation over Japan. *Hydrol Res Lett* 2:22–26. doi: [10.3178/HRL.2.22](https://doi.org/10.3178/HRL.2.22)